JAAS

PAPER

View Article Online
View Journal | View Issue

Cite this: *J. Anal. At. Spectrom.*, 2018, **33**, 809

An improved method of Cr purification for high precision measurement of Cr isotopes by double spike MC-ICP-MS

Jian-Ming Zhu, *[ab] Guangliang Wu, [a] Xiangli Wang, [cd] Guilin Han [a] and Lixin Zhang [a]

Chromium (Cr) isotopes have been used to trace pollution processes and reconstruct paleo-redox conditions. However, the precise determination of Cr isotopes is still challenged by difficulties in purifying Cr from samples with low Cr and high matrix content. Here, we developed an improved, flexible and easily operated three-step chromatographic procedure to separate Cr from high-matrix samples. A continuous, two-stage column (Step I) filled with 2 mL cation resin AG50W-X8 (200–400 m) and 2 mL anion resin AG1-X8 resin (100–200 m), followed by Step II, with 1 mL of AG1-X8 resin (200–400 m), was used to remove at least 99% of Ca, Fe, and Ti, and >90% of V and most other matrix elements, even for samples with Fe/Cr ≈ 6000 and Ti/Cr ≈ 1000. The recovery of Cr in both Step I and Step II can reach nearly 100%. Step III utilizes 2 mL AG1-X8 (100–200 m) combined with an $(NH_4)_2S_2O_8$ oxidant to remove residual matrix elements and achieve high-purity Cr. The total yield of Cr through our three-step procedure is greater than 80% even for low-Cr (2.6 μg kg^{-1}) samples. A relatively small sample amount (300–600 ng Cr) is enough to achieve high precision Cr isotope measurement due to a low procedural blank (<1 ng). Chromium isotopes in geological reference materials (BHVO-2, JDo-1, JP-1, *etc.*) were measured on a Neptune Plus MC-ICP-MS. The long-term external precision is 0.06‰ (2SD), and the δ^{53}Cr values are in great agreement with previously reported values. The δ^{53}Cr of the upper continental crust is estimated to be −0.10 ± 0.10‰ using a suite of granite, diamictite, sediment and loess samples. Both plants and human hair are ~0.1‰ heavier than the upper continental crust. Tests show that our improved purification procedure is applicable to various geological and environmental samples.

Received 4th February 2018
Accepted 27th March 2018

DOI: 10.1039/c8ja00033f

rsc.li/jaas

1. Introduction

Chromium (Cr) exists in two valence states, Cr(III) and Cr(VI), in natural environments. It has four stable isotopes, ^{50}Cr (4.345%), ^{52}Cr (83.789%), ^{53}Cr (9.501%), and ^{54}Cr (2.365%).[1] Early studies of Cr isotopes mainly focused on meteorite samples, where the ^{53}Cr–^{53}Mn system[2,3] was used as an astronomical chronometer to understand the evolution of the early solar system, due to ^{53}Mn decaying to ^{53}Cr with a short half-life (3.7 ± 0.4 Ma).[4] Recently, many studies have concentrated on the application of a stable Cr isotope system to solve paleo- and modern-environmental problems. Since Cr is a redox-sensitive element with a large Cr isotopic shift during the redox transformation between Cr(VI) and Cr(III),[5,6] Cr isotopes have become a powerful redox proxy to reconstruct the evolution of the paleo-ocean-atmosphere system.[7–9] In the modern environment, Cr is a toxic heavy metal and is widely used in electroplating, leather and dying industries. Cr pollution has attracted much attention in environmental sciences because of the carcinogenicity of Cr(VI) and its high solubility in surface waters.[10–13] In contrast, Cr(III) is insoluble in water at circumneutral pH and less toxic.[13] During the reduction of Cr(VI) to Cr(III), the δ^{53}Cr becomes systematically higher in the remaining Cr(VI) pool as reduction progresses. Therefore, Cr isotopes can be used to monitor and potentially qualify the extent of reduction in groundwater, given that isotopic fractionation factors are known (*e.g.* from experimental determinations).[5] Chromium isotopes can also be employed to trace the pollution sources and their migration paths caused by electroplating, mining, and smelting.[5,14] However, in order to understand Cr isotopic compositions in various geological reservoirs, to study Cr biogeochemical cycling in near-surface environments, and to further expand Cr isotope applications to other fields such as agriculture and soil sciences, analyzing Cr isotopic compositions with high

[a]*State Key Laboratory of Geological Processes and Mineral Resources, China University of Geosciences (Beijing), Beijing 100083, China. E-mail: jmzhu@cugb.edu.cn; Tel: +86-10-82322832*

[b]*State Key Laboratory of Environmental Geochemistry, Institute of Geochemistry, CAS, Guiyang, 550081, China*

[c]*Department of Marine Sciences, University of South Alabama, Mobile, AL 36688, USA*

[d]*Dauphin Island Sea Lab, Dauphin Island, AL 36528, USA*

precision in natural samples is a prerequisite. Chemical separation of Cr from natural samples is key to obtaining high precision isotope measurement.

In recent years, many chemical purification schemes for Cr isotope measurement have been reported[15–26] (Table 1). These methods can be divided into 2 categories according to Cr speciation and used resin types: (1) Cr is transformed to Cr(VI) by using strong oxidizing agents, and then separated from the sample matrix through an anion exchange resin;[15–17,19,21,25,26] (2) Cr(III) is converted to Cr–Cl complexes, and then separated from the matrix by using a cation exchange resin;[22] some studies treated samples with reducing agents to ensure that all Cr is in the Cr(III) state before purifying Cr using a cation resin.[18,23,24] Most of these separation schemes are limited to specific sample types such as carbonates, silicates or meteorites. Although these methods can achieve satisfactory Cr recoveries given that ^{50}Cr–^{54}Cr double spikes are added before chemical purification, their application is limited either by the long processing time or high procedural blanks for low-Cr samples. In particular, for samples with low Cr content and high levels of Fe, Mn, and Ti such as basalt BCR-2 (Fe/Cr ≈ 6000) and nodule NOD-P-1 (Mn/Cr ≈ 19 100), the reported schemes do not always achieve satisfactory Cr yields. In addition, some interference elements such as Fe and Ti can still persist after purification, which cannot meet the requirements for high-precision Cr isotope analysis. To the authors' knowledge, a universal purification protocol that is applicable to various kinds of samples and can achieve a relatively low blank and high yield has not been well developed.

This work reports an improved purification scheme for high precision measurement of Cr isotopes based on existing methods.[5,25] This scheme consists of three steps with four chromatographic columns combining anion and cation exchange resins. It can remove 100% Fe, >99% Ca, >99% Ti and >90% V in Step I and Step II, with a 100% Cr yield. In Step III, after oxidation with $(NH_4)_2S_2O_4$ and centrifugal separation of oxides formed therein, residual interfering elements are eliminated. The obtained high-purity Cr can then be used for high precision Cr isotope determination. The procedural blank for this separation scheme is lower than 1 ng, and 300–600 ng Cr (based on lab blanks) is enough to obtain enough Cr for high-precision isotope measurement (with a >80% yield) even for low-Cr samples with more complex matrices. More importantly, this scheme is simple, easy to operate, less time-consuming, and suitable for various kinds of geological or environmental samples such as minerals, rocks, soils, plants and likely meteorites. If 100% Cr is required, *e.g.* to study mass-independent Cr isotope fractionation or ^{54}Cr anomalies where double spikes cannot be used, researchers can modify Step III to achieve their special needs.

2. Experimental methods

2.1. Chemical reagents and materials

In our experiments, optima-grade HNO_3, HCl and HF, purchased from Beijing Institute of Chemical Reagents (BICR), were further distilled (twice for HNO_3 and HCl, and once for HF) using individual Savillex™ DST-4500 stills. Ultrapure water with an 18.2 MΩ cm^{-1} resistivity was obtained by using a Milli-Q Element system (Millipore, USA). High purity reagents including $(NH_4)_2S_2O_8$ (99.8%), $NH_3 \cdot H_2O$ (99.999%), hydroxylamine hydrochloride ($NH_2OH \cdot HCl$, 99.995%), 35% H_2O_2 (GR guarantee reagent) and V and Ti standard solutions (1000 μg g^{-1}) were obtained from Alfa Aesar. All PFA beakers

Table 1 Reported methods for Cr separation

Reference	Ion exchanger	Sample type	The lowest Cr concentration[a]	Yield (%)
D'Arcy *et al.* (2017)[15]	AG1-X8 (?) AG50W-X8 (200–400 m)	Carbonate	0.06	60–70
D'Arcy *et al.* (2016)[16]	AG1-X8 AG1-X8	Soil and rock Water	64	70
Gueguen *et al.* (2016)[17]	AG1-X8 (100–200 m) AG50W-X8 (200–400m)	Marine sediments	17	75–85
Bonnand *et al.* (2016)[18]	AG50W-X8 (200–400 m)	Chondrite	1410	80
Schoenberg *et al.* (2016)[19]	AG1-X8 (100–200 m) AG50W-X8 (200–400 m)	Chondrite and silicate	45.4	n.d.[b]
Schiller *et al.* (2014)[20]	AG1-X4 (200–400 m) AG50W-X8 (200–400 m) TODGA	Dunite, meteorites	n.d.	n.d.
Chrastný *et al.* (2013)[21]	AG1-X8	—	198	n.d.
Bonnand *et al.* (2011)[22]	AG50W-X8 (200–400 m)	Carbonates	1.05	70–80
Qin *et al.* (2010)[23]	AG50W-X8 (200–400 m) AG1-X8 (100–200 m)	Terrestrial rock and chondrite	280	80
Trinquier *et al.* (2008)[24]	AG50W-X8 (200–400 m)	Meteorites	n.d.	80
Schoenberg *et al.* (2008)[25]	AG1-X8 (100–200 m)	Basalt, shale, ultramafic rocks and cumulates	42.51	70–85
Halicz *et al.* (2008)[26]	AG1-X8 AG50W-X12	Silicate	320	>95

[a] The unit of concentration is μg g^{-1}. [b] No data were reported.

(Savillex™) were cleaned using HNO_3 (1 : 1), HCl (1 : 1) and MQ water. Centrifuge tubes and pipette tips were strictly cleaned before usage using 10% HNO_3, 4 M HCl and MQ water. The pretreatment of all samples was conducted in a class 1000 ultra-clean room and chemical separation was performed in a class 100 hood at the Isotope Geochemistry Laboratory of China University of Geosciences (Beijing).

2.2. Sample preparation and digestion

A series of reference materials were used to evaluate the reliability of our improved purification procedures. Several of them have published Cr isotopic compositions in previous studies, allowing cross-validation with results acquired in this work. These international geological reference materials (GRMs) include basalt (BCR-2 and BHVO-2), peridotite (JP-1), andesite (AGV-2 and GSR-2), granite (GSP-2), shale (SDo-1 and SGR-1b), carbonate (JDo-1), iron–manganese nodules (NOD-P-1 and NOD-A-1), cobalt-rich crusts (GSMC-2,-3∼3), soil (GSS-9 and GSS-11–16), stream sediments (GSD5, GSD5a, GSD7a, GSD17, GSD21 and GSD23) and animal and plant samples (GSH-1, GSV-1,-2, GSB-6 and ESP-1). These GRMs were obtained from the United States Geological Survey (USGS), Geological Survey of Japan (GSJ), Institute of Geophysical and Geochemical Research (IGGE) and China National Standard Materials Research Center (NRCCRM), respectively. Additionally, we investigated the Cr isotopic composition of the upper continental crust through loess ($n = 5$), diamictite ($n = 6$), and granite ($n = 3$) samples. Given different sample characteristics, different digestion methods were employed as follows.

2.2.1. Silicate. Typically 50 mg of basalt, andesite or granite powders were weighed into 15 mL PFA vials. Two mL HF (23 M) and 1 mL HNO_3 (15.8 M) were added. The tightly sealed PFA vials were put on a hot plate at 140 °C for at least 8 hours and sonicated for 15 minutes. The heating and sonication were repeated until the white precipitate disappeared. When the solutions were evaporated to ∼1 mL at 150 °C, they were dried down to incipient dryness at 100 °C. The samples were then treated with 3 mL of *aqua regia* ($HCl : HNO_3 = 3 : 1$) and left on a hot plate at 130 °C for more than 6 hours until the sample residue was completely dissolved. The clear sample solutions were evaporated to near dryness at 130 °C, and were finally dissolved in 1 mL 2 M HNO_3 mixed with 0.5% H_2O_2. The dissolved samples (sealed PFA vials) were left on a hot plate at 80 °C for 2 hours, and then transferred into 6 mL tubes for storage.

2.2.2. Shales and sediments. The shale, loess, soil, stream sediment and diamictite samples were digested in customized high-pressure bombs. Approximately 100 mg powders were weighed into 30 mL Teflon (PTFE) liner vials. Acids (0.5 mL HNO_3 (15.8 M) and 0.5–0.8 mL HF (23 M)) were firstly added for degassing for 1–2 h, and then 2.0–2.3 mL HNO_3 (15.8 M) was added again. The sealed bombs were put in a pre-heated oven for 36–48 h at 185 ± 5 °C. After cooling, 1 mL of 30% H_2O_2 and 0.4 mL of HF (23 M) were added. The sealed PTFE liners were carefully heated on a hot plate for 1–2 h at 130 °C, after which they were opened to allow the samples to dry down to incipient dryness. 0.1–0.3 mL HF and 3 mL HNO_3 were added to the samples to completely dissolve residues. The sealed bombs were placed in an oven again at 185 ± 5 °C for 16 h. After cooling, 1 mL of 30% H_2O_2 and 0.3 mL of HF were added to the samples and the solutions were transferred into 15 mL PFA beakers. After being heated on a hot plate at 130 °C for 2 h, the sample solutions were then evaporated to incipient dryness. Finally, the samples were dissolved in 1 mL of 2 M HNO_3 mixed with 0.5% H_2O_2.

2.2.3. Animal and plant samples. For animal and plant reference materials, typically 300 mg of masses were used. Their digestion procedures were similar to those of shales. However, 0.2 mL HF was applied only after bombs were heated in an oven at 185 ± 5 °C for 16 h. Before the bombs were placed in the oven for 16 h for the second time, only 3.2 mL of HNO_3 was added without HF. No HF was added in the subsequent steps. When the digested solutions were transferred into PFA beakers, no residue was present.

2.2.4. Carbonate and manganese nodules. For carbonates and manganese nodules, our digestion procedure slightly differs from previous methods.[22,27,28] Carbonates (JDo-1), cobalt-rich crusts (GSMC-2 and -3) and iron–manganese nodules (NOD-A-1 and NOD-P-1) were digested in bombs. 100 mg of powders were weighed into 30 mL PTFE liners, and 0.5 mL MQ water and 1 mL 6 M HCl were then added. After degassing for 2 h, the PTFE liners were put on a hot plate at 130 °C to evaporate the sample solutions to incipient dryness. 3.2 mL of concentrated HNO_3 was added to the PTFE liners, and then they were placed in a pre-heated oven at 185 ± 5 °C for 24 h. After cooling, 1 mL 30% H_2O_2 was added and transferred to 15 mL PFA beakers. The beakers were sealed and heated on a hot plate at 130 °C for 2 hours, after which they were opened and left on the hot plate to continuously evaporate the sample solutions to incipient dryness. 1 mL or 2 mL of 2 M HNO_3 mixed with 0.5% H_2O_2 was used to dissolve the samples. The digested samples, some of which contained a small amount of undissolved materials, were completely transferred into 6 mL centrifuge tubes for storage. During chromatographic separation, only the supernatant was loaded onto resins after centrifuging for 20 min at 3600 rpm.

2.3. Cr purification

An improved method for Cr purification was developed by combining cation and anion exchange resins (Table 2). Before the column chemistry for separating Cr from other matrix elements, sample aliquots containing 300 ng or 600 ng Cr were mixed with the ^{50}Cr–^{54}Cr double spike (DS) in a 15 mL PFA beaker according to the optimized ratio of $^{54}Cr_{spike}/^{52}Cr_{sample} = 0.4$. The mixed solutions were added with an appropriate amount of 2 M HNO_3 and 5 μL of 30% H_2O_2 reaching a total volume of 1 mL. The beakers containing the sample–spike mixtures were tightly sealed and placed on a hot plate overnight at 80 °C for homogenization of DS and the samples. The solutions were dried down at 100 °C and dissolved in 0.1 mL 0.5 M HCl at 80 °C for 10 minutes until clear solutions without any residue were achieved. At this time, 50 μL 100 μg L^{-1} hydroxylamine hydrochloride was added to the solutions (heating at

Table 2 Chromium purification scheme and elemental compositions in collected cuts

Separation stage	Reagent	Volume[a]
Step I		
Column 1: cation exchange resin (AG50W-X8, 200–400 mesh, 2 mL)		
Condition	10.5 M HCl	3
Load sample and collect Cr	8.5 M HCl	0.65
Collect Cr	10.5 M HCl	2
Elute Ca and Fe	5 M HNO_3	6
Column 2: anion exchange resin (AG1-X8, 100–200 mesh, 2 mL)		
Condition	6 M HCl	6
Load sample and collect Cr	6 M HCl	4.4
Collect Cr	6 M HCl	3
Elute Fe	0.3 M HCl	10
Step II		
Column 3: anion exchange resin (AG1-X8, 200–400 mesh, 1 mL)		
Condition	4 M HF	6
Load sample and collect Cr	4 M HF	2
Collect Cr	4 M HF	6
Elute Ti and V	5 M HNO_3	5
Step III		
Column 4: anion exchange resin (AG1-X8, 100–200 mesh, 2 mL)		
Condition	0.001 M HCl	10
Load sample	Neutral solution	8
Elute matrix and V	MQ	4
Elute matrix and V	0.1 M HCl	4
Elute SO_4^{2-}	2 M HCl	3.5
Elute Cr[b]	2 M HNO_3 + 0.5% H_2O_2	2
Elute Cr[b]	2 M HNO_3 + 0.5% H_2O_2	2
Elute Cr[b]	2 M HNO_3 + 0.5% H_2O_2	2
Elute Cr[b]	2 M HNO_3 + 0.5% H_2O_2	2

[a] Volume of eluent (mL). [b] Need to wait 30 min.

80 °C for 10 minutes) to ensure that all possible Cr(VI) was completely transformed to Cr(III). After cooling to room temperature, 0.5 mL 11 M HCl was added to the sample solutions and loaded onto columns. For plant and human hair samples with lower Cr contents, they were fully dissolved in 0.1 mL 0.5 M HNO_3 at 80 °C for 10 minutes, cooled to room temperature, and then neutralized with 80 μL 6.7 M ammonia hydroxide immediately before Step III purification. Step I was not performed before Step III because the hair sample could not be dissolved in 10.5 M HCl for some unknown reason. However, after Step III, the procedures specified in Step I were performed to remove Fe. Step II was skipped for human hair because of the very low amount of Ti and V.

2.3.1. Step I: two consecutive columns (1 and 2) for removing Ca and Fe. Column 1 (10 mL of a Bio-Rad polypropylene column) is loaded with 2 mL of AG50W-X8 cation resin (200–400 m, Bio-Rad), and column 2 (10 mL of a Bio-Rad polypropylene column) is loaded with 2 mL of AG1-X8 anion resin (100–200 m, Bio-Rad). The two columns were cleaned with 10 mL 5 M HNO_3, 6 mL mixed 2 M HCl and 8 M HF, and 3 mL 6 M HCl, and then washed to near neutral with MQ water. Columns 1 and 2 were conditioned with 3 mL of 10.5 M HCl and 6 mL of 6 M HCl, respectively. After conditioning, 0.65 mL of the sample mixture was loaded onto column 1, and then 2 mL (4 × 0.5 mL) 10.5 M HCl was added to the rinse resin. The obtained 2.65 mL of solution was diluted to 6 M HCl media by adding 1.9 mL MQ water. After standing for 10 minutes, it was immediately loaded onto column 2 (5 × 1 mL), followed by a 3 mL 6 M HCl rinse. All rinsing solutions in columns 1 and 2 in this step were collected because they contain Cr. Column 1 is mainly to remove Ca, Fe and some matrix elements, while column 2 is to remove residual Fe, Cu, Zn and other matrix elements. The total time for columns 1and 2 is less than 2 h and operation is relatively simple. Finally, 5 M HNO_3 and MQ water were used to clean the resin for reuse. No obvious column memory effect was found in our scheme, as shown by very low Cr (0.04 ng) rinsed from reused columns.

2.3.2. Step II: column 3 for removing Ti and V. Column 3 mainly removes Ti, V and some Mg. The eluent in Step I was dried down and dissolved in 0.05 mL (for high-Cr samples) or 0.1 mL (for lower Cr samples such as BCR-2) 0.5 M HNO_3, and left on a hot plate at 80 °C for 10 minutes to ensure a clear solution, and then 10 uL of 100 μg g^{-1} hydroxylamine hydrochloride was added and the samples continue to be heated at 80 °C for 10 minutes to fully convert Cr into the Cr(III) form. After cooling, 2 mL 4 M HF was added to the samples. The samples were then loaded by the way of 2 × 1 mL onto column 3 filled with 1 mL of AG1-X8 anion resin (200–400 m, Bio-Rad), which was pre-cleaned using the same protocol as Step I and preconditioned with 6 mL 4 M HF. The resin was rinsed with additional 4 mL 4 M HF by the way of 8 × 0.5 mL. All eluents in Step II were collected. The time consumption of this step was approximately 1.5 hours. For carbonate rocks, Step II was skipped.

2.3.3. Step III: column 4 for obtaining high-purity Cr. Step III mainly eliminates residual interference and matrix elements such as Mn, Al, and Mg and a very small amount of Ti and V. After the collected eluents containing Cr in Step II were evaporated to dryness on a hot plate, 0.05 mL 0.5 M HNO_3 was added to completely dissolve the sample, and then 10 μL 6.7 M $NH_3 \cdot H_2O$, 0.5 mL 0.2 M $(NH_4)_2S_2O_8$ and 4.44 mL MQ water were added to make a solution of 5 mL 0.02 M $(NH_4)_2S_2O_8$ in neutral to alkalescent media. The samples were then placed on a hot plate at 140 °C for 3 h. The occurrence of manganese oxide precipitation indicated that all Cr(III) was transformed into Cr(VI), and the whole sample was transferred to a 6 mL centrifuge tube. 1 mL MQ water was used to rinse the PFA beaker and the rinse was combined with the corresponding samples. The tube was centrifuged at 3600 rpm for 20 minutes, and then the supernatant was transferred to the original PFA beaker. The centrifuge tubes were rinsed with 2 mL MQ water in a vortex mixer, centrifuged again, and the supernatant was combined with the original samples. If there was no precipitate, 3 mL of MQ water was added to the PFA beaker to match the 8 mL of those samples that have precipitates. The column 4 protocol is the same as the column 2 protocol except that the preconditioning acid used was 6 mL 0.001 M HCl. The sample was loaded onto the column (8 × 1 mL), rinsed with 4 mL MQ water (4 × 1 mL), 4 mL 0.1 M HCl (4 × 1 mL), and 3.5 mL 2 M HCl (7 × 0.5 mL). Finally, 2 M HNO_3 doped with 0.5% (v/v) H_2O_2 was added (4 × 2 mL) with an interval of 30 min to reduce and elute

Cr, and was collected in clean PFA beakers. The total processing time for this step was about 8 h.

For carbonate rocks, incomplete removal of a large amount of Ca and Mg will lead to clogging of resin in column 3 due to the formation of fluorides. Therefore, Step II was skipped for carbonates. However, the recovery of Cr in this scheme is still high, ranging from 80% to 98%, and Ca, Ti and V can be removed in Step III. After drying down, the pure Cr spot was dissolved in 2 mL 2.5% HNO_3 (ref. 29) for isotope measurement.

2.4. Analysis of Cr isotopes

2.4.1. Cr double spike. The ^{50}Cr–^{54}Cr double spike was used to correct isotope fractionation caused by chemical separation and instrumental mass bias.[5–9,14,23,25,27,28] Single spikes of ^{50}Cr and ^{54}Cr were purchased from ISOFLEX (USA), and they were mixed and their isotopic ratios were calibrated on a MC-ICP-MS (Nu Plasma) at the University of Illinois at Urbana-Champaign. In order to achieve high precision Cr isotope measurement, the ratio of $^{54}Cr_{spike}$ to $^{52}Cr_{sample}$ was optimized using a Monte Carlo-Nest Iterative method, whose mathematical principle was similar to that demonstrated by John *et al.* (2012)[30] and Rudge *et al.* (2009).[31] As shown in Fig. 1, given that $^{50}Cr : {}^{54}Cr = 1.30557$, the optimal mixing ratio of $^{54}Cr_{spike}$ to $^{52}Cr_{sample}$ should be in the range of 0.2–2.0, and a $^{54}Cr_{spike}/^{52}Cr_{sample}$ ratio of 0.4 was selected in our study. Our tests using underspiked, normal and overspiked samples confirm the theoretical estimates of errors (Fig. 1).

2.4.2. Mass spectrometry. The chromium isotopic composition was determined on two Neptune Plus MC-ICP-MSs (Thermo Fisher) at the Isotope Geochemistry Laboratory, China University of Geosciences (Beijing) and Beijing Createch Testing Technology Co. Ltd. Both instruments are equipped with 9 Faraday cups, each with a 10^{11} Ω amplifier. The measurement was conducted in static mode using seven Faraday cups (Table 3): ^{50}Cr (L2), ^{52}Cr (C), ^{53}Cr (H1), ^{54}Cr (H2), ^{49}Ti (L3), ^{51}V (L1), and ^{56}Fe (H4). ^{49}Ti, ^{51}V, and ^{56}Fe were detected to monitor and correct the isobaric interference of ^{50}Ti–^{50}V on ^{50}Cr and ^{54}Fe on ^{54}Cr. In order to improve the signal intensity of ^{52}Cr and to minimize $^{40}Ar^{16}O^+$, $^{40}Ar^{14}N^+$ and some oxide/nitride interference, the combination of an H cone (sample cone) and X cone (skimmer cone) was applied. Medium (MR: $M/\Delta M = 6500$) or high-resolution mode (HR: $M/\Delta M \geq 8500$) (depending on the shoulder peak plateau at MR, Fig. 2) was used in order to eliminate polyatomic interferents including $^{40}Ar^{12}C^+$, $^{40}Ar^{16}O^+$, and $^{40}Ar^{14}N^+$ and other interferents as described in previous studies.[22,25,27,28]

Table 3 The instrument operating parameters for Cr isotope composition measurement

Parameters	Wet plasma
Cup configuration	L3 (^{49}Ti), L2 (^{50}Ti, ^{50}V, ^{50}Cr), L1 (^{51}V), C (^{52}Cr), H1 (^{53}Cr), H2 (^{54}Fe, ^{54}Cr), H4 (^{56}Fe)
RF power	1250 W
Cooling gas	15 L min^{-1}
Auxiliary gas	0.80 L min^{-1}
Sample gas	1.05 L min^{-1}
High vacuum	1.2×10^{-8} Pa
Medium/high resolution	≥6500/8500
Sample uptake	50 μL min^{-1}
Cones	H (sample cone), X (skimmer cone)
Sensitivity	15 V ppm^{-1} for MR and 10V ppm^{-1} for HR

Measurements were usually conducted at concentrations of 250 (for MR) to 300 (for HR) ng mL^{-1}. The samples were injected into the plasma through a quartz spray-chamber connected to a PFA aspiration nebulizer with an uptake of 50 μL min^{-1} *via* a Cetac ASX-112FR automatic sampler. The samples were dissolved in 2.5% (v/v) HNO_3. Before each analytical session, instrumental parameters were tuned to ensure the strongest signal intensity of ^{52}Cr (central cup), which was generally 15 V ppm^{-1} at MR and 10 V ppm^{-1} at HR. Cr isotope and ^{49}Ti, ^{51}V and ^{56}Fe signals were collected at the flat part of the peak shoulder (Fig. 2) as suggested by Dauphas *et al.* (2009)[32] and He *et al.* (2015).[33] Signals were collected for three blocks, each block with 20 measurement cycles, each cycle with 4 s integration time. The total time for each sample measurement was approximately 10 min including the washing time. Before analyzing every sample and standard NIST 979, the sample introduction system was washed with 2.5% HNO_3 for 2–3 min until the ^{52}Cr signal reduces to ~1.2 mV. The blank of 2.5% HNO_3 was then measured at the peak and subtracted from subsequent sample signals. The spiked standard NIST 979 was measured before and after every 3–5 samples to monitor the stability of the instrument.

Data reductions were performed offline using an iterative method adapted from previous work.[34] Cr isotopic ratios were reported relative to the isotopically certified NIST 979 in the delta notation as previous studies: $\delta^{53}Cr$ (‰) = $(((^{53}Cr/^{52}Cr)_{sample}/(^{53}Cr/^{52}Cr)_{NIST\ 979} - 1) \times 1000$. During our measurement, the $\delta^{53}Cr$ of spiked NIST 979 typically has a small offset less than 0.12‰ due to instrument's mass bias and exponential law used.

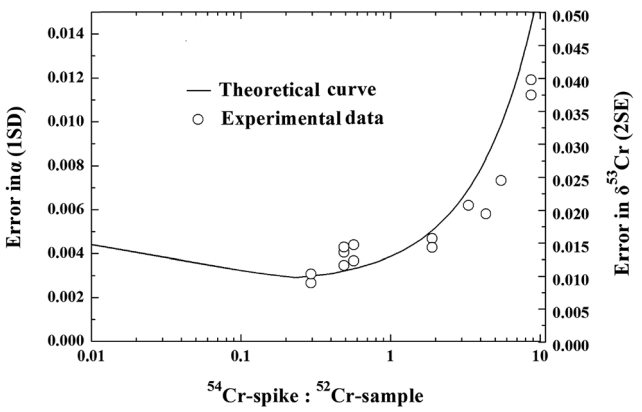

Fig. 1 Comparison between theoretically simulated and measured errors is to achieve the best mixing ratio at different ^{54}Cr-spike/^{52}Cr-sample ratios. α refers to the mass fractionation factor of natural samples relative to NIST 979. The right *y*-axis represents the variation of the 2 standard error of $\delta^{53}Cr$ analyzed at different ratios of spike to sample.

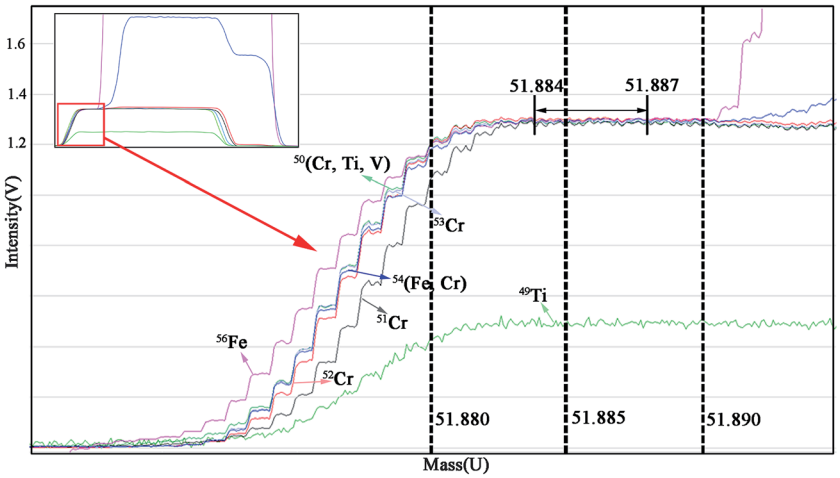

Fig. 2 A peak scan of the tuning solution containing 95 ng mL^{-1} Cr showing the platform of measuring Cr isotopes, ^{49}Ti, ^{51}V and ^{56}Fe under medium resolution mode on a Neptune Plus MC-ICP-MS.

Sample δ^{53}Cr values were normalized to the average of bracketing NIST 979 standards: $\delta^{53}Cr_{corrected\ sample} = \delta^{53}Cr_{sample} - \delta^{53}Cr_{NIST\ 979}$.

3. Results and discussion

3.1. Cr recovery

The speciation of Cr is critical for achieving high recovery.[29,35] In HCl, Cr(III) occurs as Cr^{3+}, $CrCl^{2+}$, $CrCl_2^{+}$ and $CrCl_3$. In near neutral solutions, Cr(VI) is stable as CrO_4^{2-} and $HCrO_4^{-}$.[29] Given the various types of samples and digestion methods used in our work, Cr may be present as different species (Cr(III) and Cr(VI)) in the digestion solution. To achieve a high yield, the digested samples were stored in 2 M HNO_3 mixed with 0.5% H_2O_2 before chemical separation for at least 5 days to ensure that all Cr was transformed into Cr(III).[29] Meanwhile, 10–50 μL 100 μg mL^{-1} hydroxylamine hydrochloride was added to the sample to prevent the possible formation of Cr(VI) during drying down before loading onto columns. However, we still found that the recovery of Cr during purification was influenced by the storage time of digested solutions. As listed in Table 4, the four BHVO-2 were stored for more than 5 days after digestion, and the average recovery of Cr was 84%. The last one was immediately processed to purify and the Cr yield was only 74%. This phenomenon was also observed for other samples such as SGR-1b and GSS-11 (Table 4) with 65% and 63% recoveries, respectively, which confirmed the observation in Larsen *et al.* (2016)[29] that all Cr stayed as Cr(III) when stored in nitric acid media for more than one week. Consequently, the digested sample solutions in our experiment are usually stored for 5 days at room temperature before ion exchange chromatography.

A good purification scheme should not only achieve high Cr recovery, but also eliminate isobaric and matrix interference. Among previously reported purification procedures, Cr-oxidation using a strong oxidant such as $K_2S_2O_8$, $(NH_4)_2S_2O_8$ and $KMnO_4$ is the most common one.[25–28] The oxidation strategy is effective for samples with high Cr, and lower Fe and Mn, and the yield of Cr is high. However, for low-Cr samples, especially with high Fe, Mn or Ti (*e.g.* BCR-2 or NOD-P-1), the Cr yield by the oxidation strategy is not satisfactory (Table 4), and interference elements such as Ti, Fe and V cannot be completely removed. It was found in our experiment that the precipitate produced from Cr-oxidation was mainly composed of Fe, Mn, Ti and V, which accounted for 90%, 95%, 99% and 75% in the original solution, respectively. This suggests that most interfering elements Fe, Ti and V were removed in the oxidation procedure. For the same amount of Cr at 600 ng, the precipitate for BCR-2 was far more than BHVO-2. The Cr content of the precipitate for BCR accounts for 15% of the total Cr, while the latter is only 2%, suggesting that the loss of Cr during precipitation is more severe for samples with low Cr/matrix ratios. In order to solve the low recovery problem for low-Cr samples, Fe, Ti, and other matrix elements need to be removed first to reduce the amount of precipitate.

In previous studies, 6 M HCl was used to remove Fe through AG1-X8/X4 anion resin.[5,16,19,20,23,25,35,36] This procedure can be complicated by several factors: (1) for samples with high Fe such as BIF and Fe–Mn nodules, iron can overload columns and result in the loss of Cr (unless very large resin volumes are used); (2) for samples with low Cr content, the recovery of Cr is low, as shown by BCR-2 investigated in this work, with a yield of only 75%. To achieve full recovery, the eluent volume would be too large. In addition, the subsequent procedure of using HF to remove Ti and V will also easily lead to the blockage of the column owing to the presence of high Ca, which further decreases the Cr recovery. Therefore, two consecutive columns (Step I), with 2 mL of AG50W-X8 and 2 mL of AG1-X8 resin, were employed to effectively remove Ca and Fe, even for carbonates and BIF. In 10.5 M HCl as the eluant, 80% Fe, 99% Ca and some matrix elements were adsorbed on AG50W-X8 resin, similar to AG50W-X4 cation resin reported by Wombacher *et al.* (2009),[37] while all Cr(III) passes through. The collected 10.5 M HCl eluant was diluted to 6 M HCl with MQ water and immediately loaded onto AG1-X8 columns, with the remaining Fe and some matrix

Table 4 Cr isotopic composition of geological standards in this study and in the literature

Sample name	Sample type	Reference	Cr (μg g^{-1})	Ti/Cr	Fe/Cr	δ^{53}Cr	2SD	N^a	Ti/Cr after purification	Fe/Cr after purification	Yield
JP-1	Peridotite	This study	2800	0.13	22	−0.05	0.06	3	<0.01	0.02	92%
		Schoenberg *et al.* (2016)[19]				−0.067	—				
		Li *et al.* (2016)[27]				−0.112[b]	—				
		Bonnand *et al.* (2016)[18]				−0.128	0.02				
		Bonnand *et al.* (2016)[43]				−0.102	0.012				
BHVO-2	Basalt	This study	305	53	283	−0.12	0.02	3	0.01	0.01	85%
						−0.15	0.04	3	0.01	<0.01	90%
						−0.13	0.03	3	<0.01	<0.01	81%
						−0.11	0.06	3	<0.01	<0.01	81%
						−0.09	0.06	3	<0.01	<0.01	74%[d]
Average						−0.12	0.04	15			84%
		Schoenberg *et al.* (2008)[25]				−0.126	0.084	3			
		Li *et al.* (2016)[27]				−0.155	—	—			
		Schoenberg *et al.* (2016)[19]				−0.178	—	—			
		Wang *et al.* (2016)[42]				−0.11	0.08	7			
		Wu *et al.* (2017)[46]				−0.09	0.03	8			
BCR-2	Basalt	This study	16.0	844	6038	−0.11	0.05	3	0.02	<0.01	91%
						−0.081	0.06	1	0.02	0.01	85%
						−0.072	0.06	1	0.04	0.01	85%
Average						−0.09	0.06	3	—	—	87%
GSR-3	Basalt	This study	152	93	1006	−0.19	0.02	3	<0.01	<0.01	80%
GSR-2	Andesite	This study	32.0	97	1653	−0.12	0.02	3	<0.01	<0.01	79%
AGV-2		This study	16.9	226	2769	−0.14	0.04	4	<0.01	<0.01	82%
GSP-2	Granodiorite	This study	18.6	215	1844	−0.10	0.02	3	<0.01	<0.01	81%
LN2-58[c]	Biotite granite	This study	2.60			−0.13	0.06	3			76%
GSMC-2	Cobalt-rich crust	This study	12.7	902	8514	−0.32	0.04	3	<0.01	<0.01	83%
GSMC-3		This study	11.5	998	9059	−0.37	0.04	3	<0.01	<0.01	89%
NOD-A-1	Manganese nodule	This study	27.9	115	3918	0.03	0.04	3	<0.01	<0.01	71%
		Gueguen *et al.* (2016)[17]				0.07	0.09	16			
NOD-P-1		This study	15.2	199	3910	−0.08	0.06	3	0.02	<0.01	75%
JDo-1	Carbonatite	This study	7.1	—	100	1.64	0.06	3	<0.01	0.06	85%
		Bonnand *et al.* (2011)[22]				1.72	0.059	10			
		Rodler *et al.* (2016)[40]				1.69	0.05	10			
		Pereira *et al.* (2016)[44]				1.70	0.085	5			
		Gilleaudeaur *et al.* (2016)[45]				1.64	0.03	3			
		Li *et al.* (2016)[27]				1.643[b]	0.054	10			
14ZK-77[c]	Diamictite	This study	45.5			−0.09	0.04	3			
14ZK-86[c]		This study	51.7			−0.06	0.03	3			
14ZK-186[c]		This study	39.2			−0.06	0.06	3			
14ZK-188[c]		This study	46.2			−0.09	0.06	3			
Mozaan[c]		This study	334			−0.12	0.06	3			
Timeball[c]		This study	123			−0.10	0.06	3			
GSD5	Stream sediment	This study	67.9	79	710	−0.19	0.03	3	0.02	0.3	98%
GSD5A		This study	67.0	69	641	−0.14	0.01	3	0.02	<0.01	95%
GSD7A		This study	45.6	90	775	−0.14	0.03	3	0.021	<0.01	71%
GSD17		This study	34.5	85	1344	−0.07	0.03	3	<0.01	0.02	81%
GSD21		This study	32.5	101	1124	−0.17	0.02	3	0.02	<0.01	96%
						−0.16	0.03	3	0.02	<0.01	94%
Average						−0.17	0.06	2	—	—	95%
GSD23		This study	74.3	61	779	−0.10	0.06		<0.01	<0.01	81%

Table 4 (*Contd.*)

Sample name	Sample type	Reference	Cr (μg g^{-1})	Ti/Cr	Fe/Cr	δ^{53}Cr	2SD	N^a	Ti/Cr after purification	Fe/Cr after purification	Yield
SGR-1b	Shale	This study	32.3	8	657	0.29	0.03	3	<0.01	<0.01	85%
						0.30	0.05	3	0.01	<0.01	84%
						0.31	0.05	3	<0.01	<0.01	81%
						0.30	0.04	3	<0.01	<0.01	65%[d]
Average						0.30	0.06	4	—	—	83%
SDo-1		This study	55	78	1189	−0.092	−0.03	4	<0.01	0.02	84%
						−0.088	−0.02	4	<0.01	0.02	83%
Average						−0.09	0.06	2	—	—	84%
		Schoenberg *et al.* (2008)[25]				−0.08	0.048				
GSS-8	Loess	This study	68.0	56	601	−0.12	0.06	3	<0.01	0.07	86%
HT-1[c]		This study	65.7	57	463	−0.12	0.04	3	<0.01	0.02	89%
HT-2[c]		This study	53.5	56	428	−0.05	0.03	3	<0.01	0.02	82%
HT-3[c]		This study	94.3	54	446	0.00	0.06	3	<0.01	0.02	88%
HT-4[c]		This study	102.5	50	446	−0.01	0.08	3	<0.01	0.04	94%
GSS9	Soil	This study	73.6	58	604	−0.11	0.04	3	0.02	<0.01	98%
GSS11			62.5	63	583	−0.12	0.06	3	<0.01	<0.01	83%
						−0.15	0.04	3	0.01	0.02	63%[d]
Average						−0.14	0.06	2	—	—	83%
GSS12		This study	64.3	61	681	−0.11	0.04	3	0.02	<0.01	90%
						−0.10	0.06	3	0.02	<0.01	80%
Average						−0.10	0.06	2	—	—	85%
GSS13		This study	74.3	51	516	−0.10	0.05	4	<0.01	<0.01	80%
						−0.11	0.02	4	0.01	<0.01	90%
Average						−0.11	0.06	2			85%
GSS14		This study	70.8	57	614	−0.12	0.06	3	0.02	<0.01	98%
GSS15		This study	93.3	56	571	−0.10	0.06	3	<0.01	<0.01	84%
GSS16		This study	67.1	86	660	−0.08	0.04	3	<0.01	<0.01	83%
GSH-1	Human hair	This study	0.41	6.58	132	−0.03	0.06	3	<0.01	0.02	70%
GSB-6	Spinach	This study	1.37	20.4	394	−0.01	0.06	3	<0.01	0.20	73%
GSV-1	Shrub leaf	This study	2.18	41.8	469	−0.04	0.06	3	<0.01	0.06	97%
GSV-2		This study	2.57	37.0	417	−0.06	0.06	3	<0.01	0.06	99%
ESP-1	Tomato leaf	This study	3.93	21.2	316	−0.04	0.06	3	<0.01	0.26	79%

[a] The times of repeated measurements of the same solution by MC-ICP-MS. [b] The data were reported by 2SE. [c] The samples were obtained from other researchers; they were not reference materials. [d] The sample was immediately processed after digestion.

elements such as Cu, Co and Zn adsorbed. All Cr(III), Mn, and Ti, and some V, Mg and other matrix elements pass through the resin and were collected. In these two columns, the recovery of Cr can reach nearly 100%, and most of the matrix elements can be removed, whereas the processing time is less than 3 h, significantly improving the column efficiency.

Diluted HF is generally utilized to separate V and Ti with AG1-X8 and Ln Spec resin, except for Schiller *et al.* (2014)[20] who used TODGA to remove Ti and V in 14 M HNO_3 and 8 M HCl. Another resin used to remove Ti is AG50W-X8 resin.[22] Zhang *et al.* (2011)[38] reported that V and Ti can be effectively adsorbed on AG1-X8 resin in 4 M HF. In our scheme, using 4 M HF as the eluant, 99% Ti and >90% V can retain on the resin, while 100% Cr(III) and most Mn and Mg immediately rinse out. The processing time for this column procedure is approximately 2 h. However, we note that this step works well because >99% Ca was removed in Step I. In comparison with other schemes,[27] this step is simple and easy to operate.

In Steps I and II, the yield of Cr is 100%. Only Mn, Mg, Al, and K and a small amount of V are still present in the collected eluents. The following Step III can be flexible depending on specific needs. According to Bizzarro *et al.* (2011),[39] Mn can be effectively removed through AG50W-X8 by using the mixture of 0.5 M HCl and 95% acetone, but Cr and V cannot be separated. According to Larsen *et al.* (2016),[29] a high yield (>90%) and cleaner Cr can be obtained using AG50W-X8 resin. However, considering the long time (18 h at 145 °C) needed for Cr species transformation in concentrated HCl media,[29] we adopted a simple Step III to separate Cr. When Cr(III) was oxidized to Cr(VI) with $(NH_4)_2S_2O_4$ under neutral or alkaline conditions (pH $\leq$ 9), Mn (>95%), V (>9%) and Cr (~1%) are sequestered by precipitates and removed by centrifugation. But for Fe–Mn nodules, there is still ~15% Cr lost because of too much precipitates formed. This indicates that the amount of precipitate may affect the Cr recovery. In order to further reduce the loss of Cr during rinsing after loading samples onto the resin, we used 4 mL MQ and 4 mL 0.1 M HCl water instead of 8–10 mL 0.1 M HCl to elute residual elements such as V, Al, Mg and K, and 3.5 mL of 2 M HCl to completely elute SO_4^{2-} produced in the oxidation process. Our tests found that ~2% and ~7% of Cr were lost during the water rinse and HCl rinses, respectively. Recently, Li *et al.* (2017)[28] proposed $KMnO_4$ as an oxidant and

obtained a >95% Cr yield. However, this method is unsuitable for low-Cr samples such as granite and Fe–Mn nodules. Interestingly, there is no Cr loss during 0.2 M and 4 M HCl rinsing after sample loading, which is significantly different from our result that the loss of Cr is at least 2–7% even when using MQ water and 2 M HCl. We think that one reason for the difference is that the yield of Cr is related to the properties of samples. Another reason may be that 20 mM $(NH_4)_2S_2O_4$ was used instead of 2 or 5 mM suggested by Li *et al.* (2016),[27] which means that the more SO_4^{2-} formed in our experiment affects the Cr recovery.

For carbonate and other samples with high Ca and Mg contents, Step I cannot remove all Ca and Mg. Fluorides such as CaF_2 and MgF_2 will be formed in Step II and block the column. Therefore, for these samples Step II is omitted. The combination of Steps I and III can obtain relatively pure Cr due to low Ti and V contents in carbonates. If necessary, the column order can be adjusted to Step I, Step III and Step II, which still works well.

3.2. Evaluation of isobaric interference

Generally, there are two kinds of interferents during Cr isotope measurement using MC-ICP-MS. One is polyatomic interferents such as $^{36}Ar^{14}N^+$, $^{40}Ar^{12}C^+$, $^{36}Ar^{16}O^+$, $^{40}Ar^{13}C^+$, $^{36}Ar^{16}O^1H^+$, $^{40}Ar^{14}N^+$ and $^{40}Ar^{16}O^+$, which are formed in the ionization process. The other kind is isobaric interferents such as ^{54}Fe, ^{50}Ti, and ^{50}V. In order to eliminate these interferents, our Cr isotope measurements, following previous studies,[22,25,26,35] were carried out in the medium or high resolution mode. As shown in Fig. 2, ^{56}Fe and $^{40}Ar^{16}O^+$, and ^{52}Cr and $^{36}Ar^{16}O^+$ can be separated in the medium resolution mode. Isobaric interferents (^{54}Fe on ^{54}Cr and ^{50}Ti–^{50}V on ^{50}Cr) can be subtracted by measuring ^{56}Fe, ^{49}Ti and ^{51}V and using assumed $^{56/54}Fe$, $^{49/50}Ti$, and $^{51/50}V$ ratios. However, this mathematical subtraction is effective only when such interferents are relatively low, and Fe–Ti–V in samples has the assumed $^{54}Fe/^{56}Fe$, $^{49}Ti/^{50}Ti$, and $^{51}V/^{50}V$ ratios. High levels of these interference elements relative to Cr in samples can lead to wrong $\delta^{53}Cr$ values. In order to evaluate the effect of isobaric interference, different amounts of Ti and Fe (ICP-MS standard solution from Alfa Aesar) were added to two NIST 979 solutions of the same amount to achieve a range of Ti/Cr and Fe/Cr, and then Cr isotopic composition was analyzed. Several observations can be made from the results shown in Fig. 3: (1) the effect of Ti and Fe on the $\delta^{53}Cr$ has the same trend: more interference elements lead to higher $\delta^{53}Cr$, and the effect of Ti is relatively more obvious than that of Fe. This observation is consistent with Bonnand *et al.* (2011);[22] (2) high Ti/Cr and Fe/Cr ratios lead to incorrectly high $\delta^{53}Cr$ values; when the ratios of Ti/Cr and Fe/Cr are less than 0.3 and 0.4, there is no effect on $\delta^{53}Cr$. In our original samples, although Ti/Cr and Fe/Cr are greater than 1000 (Fe/Cr as high as 9000), the Ti/Cr and Fe/Cr can be reduced to <0.01 and 0.1, respectively, after purification using our improved separation scheme. This confirms that our improved procedure is suitable for low-Cr samples with complex matrices.

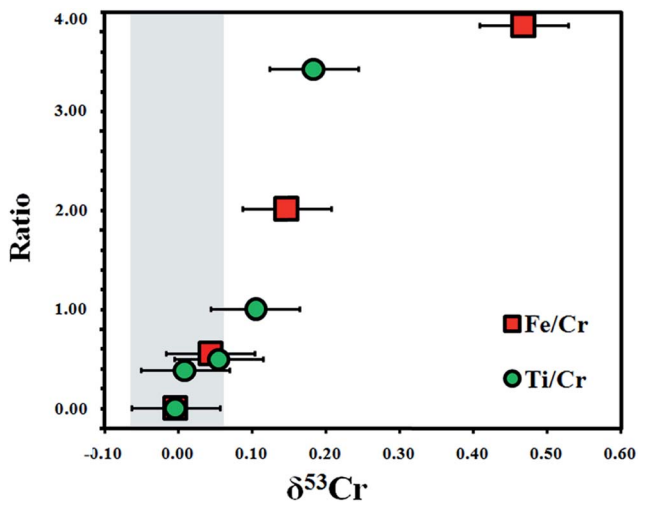

Fig. 3 The effect of various amounts of interfering elements on measured $\delta^{53}Cr$.

3.3. Blank, precision and accuracy

3.3.1. Blank contribution. The total procedural blank of Cr, including digestion in PTFE vessels and all columns, ranges from 0.6 ng to 1 ng, which is similar to the lowest blank level achieved in previous studies.[24,25,40,41] We did not obtain a 0.15 ng Cr blank reported by Li *et al.* (2017),[28] even though we eliminated "the memory effect of column" suggested by Pontér *et al.* (2016).[35] The effect of the Cr blank was assessed by mixing a blank solution with spiked NIST 979, and the measured $\delta^{53}Cr_{NIST\ 979}$ is identical within uncertainty to that of the pure NIST 979 solution. Since Cr in our sample for isotope measurement is generally 250 ng mL^{-1}, which is similar to that in the test NIST 979, the effect of the blank (from chemical reagents and procedures used in this study) on our samples is negligible. Additionally, using our proposed cleaning procedure, the column memory effect was not found in the reused resin, in contrast to the column memory effect reported by Pontér *et al.* (2016).[35] However, the resin was discarded after being used six or seven times, because we observed that the Cr yield gradually decreased to <60% or lower.

3.3.2. The precision and accuracy of Cr isotope measurement. Fig. 4 presents the long-term external precision of unprocessed and processed NIST 979, as well as unprocessed NIST 3112a reported over the past two years. Each measurement was normalized to bracketing standard NIST 979. The precision was better than 0.04‰ (2SD) based on NIST 979 and NIST 3112a. In order to further evaluate the precision of actual samples, geological standard materials (GSMs) including BHVO-2 (305 μg g^{-1}), BCR-2 (16 μg g^{-1}) and SGR-1b (32.3 μg g^{-1}) were digested multiple times. Their external precision was 0.04 (2SD, $n = 5$), 0.06 (2SD, $n = 3$) and 0.06 (2SD, $n = 4$), respectively (Table 4), the same as those measured on TIMS and MC-ICP-MS in previous studies.[20,22,25,27,28,42] These results suggest that our purified samples are clean and the whole process (sample digestion, chemical separation and isotope measurement) is highly reproducible.

The accuracy of our method was evaluated by analyzing standard solution NIST 979, NIST 3112a and GSMs, all with well

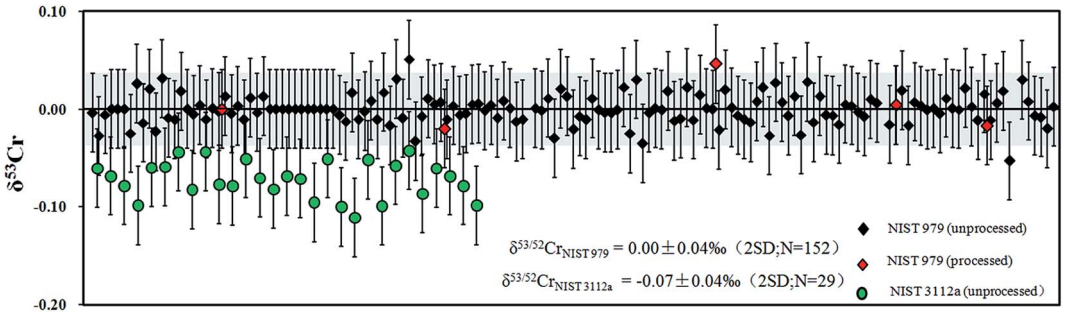

Fig. 4 The long-term reproducibility of δ^{53}Cr for NIST 979 and NIST 3112a. Dark diamond represents unprocessed NIST 979; red diamond represents processed NIST 979 (600 ng); green circle represents unprocessed NIST 3112a.

known δ^{53}Cr values. The long-term results for NIST 979 and NIST 311a are 0.00 ± 0.04‰ (2SD; n = 152) and −0.07 ± 0.04‰ (2SD; n = 14), respectively. NIST 979 solution containing 300–600 ng Cr was processed through the procedures the same way as the samples, and the result is 0.00 ± 0.05‰ (2SD; n = 5), consistent with previously reported values.[22,25,26,40] As shown in Table 4, repeatedly digested and analyzed BHVO-2, SDo-1, JP-1, and JDo-1 return δ^{53}Cr values of −0.12 ± 0.06‰ (2SD; n = 15), −0.05 ± 0.06‰ (2SD; n = 3), −0.09 ± 0.06‰ (2SD; n = 8), and 1.64 ± 0.06‰ (2SD; n = 3), respectively. Li *et al.* (2016)[27] and Bonnand *et al.* (2016)[18,22,43] reported that the Cr isotopic composition of JP-1 and JDo-1 analyzed by TIMS is −0.112 ± 0.022‰ (2SE; n = 3), −0.128/−0.102 ± 0.02‰ (2SD), 1.643 ± 0.054‰ (2SE; n = 10), and 1.72 ± 0.059‰ (2SD; n = 10), respectively. δ^{53}Cr in JDo-1 determined by Pereira *et al.* (2015)[44] and Gilleaudeaur *et al.* (2016)[45] is 1.70 ± 0.054‰ (2SD; n = 5) and 1.64 ± 0.03‰ (2SD; n = 3). δ^{53}Cr in BHVO-2 reported by Schoenberg *et al.* (2008),[25] Wang *et al.* (2016),[42] and Wu *et al.* (2017)[46] is −0.126 ± 0.084‰ (2SD; n = 3), −0.11 ± 0.08‰ (2SD; n = 7) and −0.09 ± 0.03‰ (2SD; n = 8). Our results are in great agreement with the published data (Fig. 5).

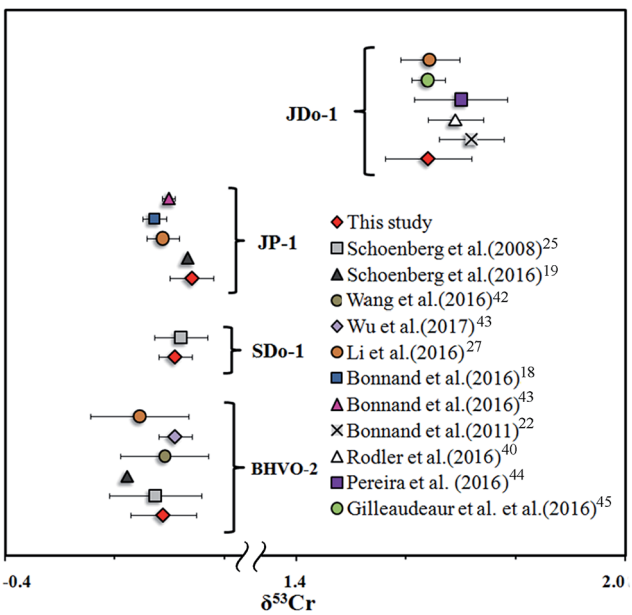

Fig. 5 δ^{53}Cr values in selected geological reference materials measured in this work *versus* previous studies.

3.4. Cr isotopes in geological and environmental reference materials

Apart from the aforementioned BHVO-2, JP-1, SDo-1 and JDo-1, the Cr isotopic composition in some magmatic rock samples including ultrabasic (JP-1), basic (BCR-2 and GSR-3), intermediate igneous rocks (AVG-2 and GSR-2) and felsic magmatic rocks (GSP-2) was also measured. The δ^{53}Cr values in GSR-3, AVG-2, BCR-2, GSR-2 and GSP-2 were reported for the first time to be −0.09 ± 0.06‰, −0.19 ± 0.06‰, −0.14 ± 0.06‰, −0.12 ± 0.06‰ and −0.10 ± 0.06‰, respectively. A limited δ^{53}Cr range from −0.09 to −0.19 with an average of −0.13 ± 0.06‰ was observed, and it was similar to that of bulk earth silicate (BSE) reported by Schoenberg *et al.* (2008)[25] (−0.124 ± 0.101‰) and Xia *et al.* (2017)[47] (−0.14 ± 0.12‰). These results were interpreted as evidence for a relatively homogeneous Cr isotope composition for the mantle and almost no Cr isotopic fractionation during partial melting and magma differentiation.

Shale has become an important archive for using δ^{53}Cr to reconstruct the redox evolution of paleo-oceans.[8] The Cr isotopic compositions of two international shale GSMs (SGR-1b and SDo-1) were determine to be 0.30 ± 0.06‰ and −0.09 ± 0.06‰, respectively. However, a large range of Cr isotopic composition (0.02 ± 0.08‰ to 1.8‰) was observed in shales from different geological times by recent work.[8,42] The large fractionation is thought to reflect the redox state of the ocean-atmosphere system. Since SDo-1 has been discontinued, SGR-1b could be used as a reference material for interlaboratory comparison.

Soils, stream sediments and loess are important geological reservoirs of Cr in the upper continental crust,[48,49] and understanding their Cr isotope systematics is important for understanding the global Cr cycle in the surface environment. In this study, Cr isotopic compositions of seven soils and six stream sediments collected from different provinces of China by IGGE were also reported for the first time. The mean δ^{53}Cr is −0.11 ± 0.03‰ for soils, −0.13 ± 0.08‰ for stream sediments, and −0.09 ± 0.05‰ for loess (n = 5), suggesting that the Cr isotope composition in these sediment types is fairly uniform and is

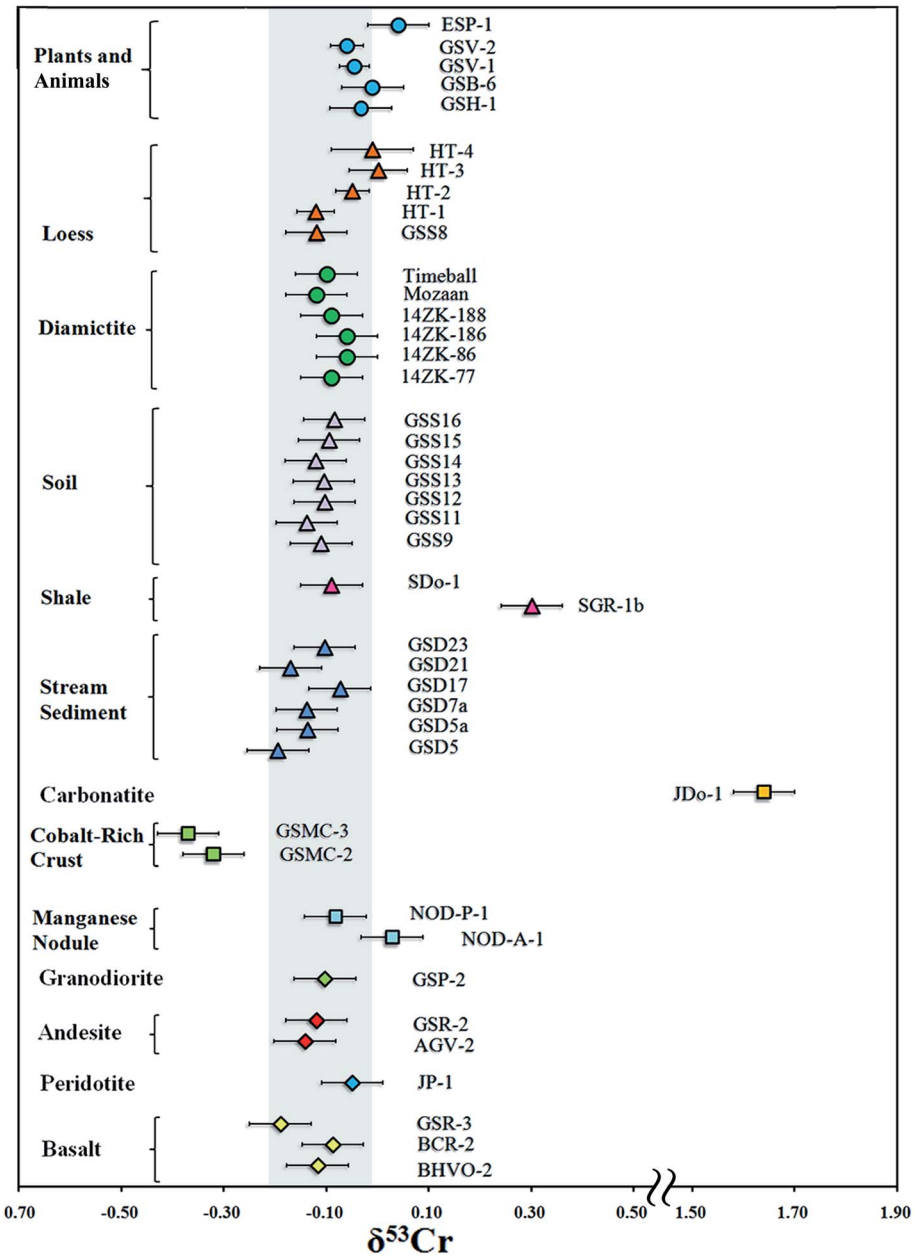

Fig. 6 δ^{53}Cr values in some geological reference materials and selected geological samples.

within uncertainty the same as that of the bulk silicate Earth ($-0.124 \pm 0.101‰$).[25]

Although previous studies have estimated the δ^{53}Cr of the bulk silicate Earth, no estimates exist for the upper continental crust. According to the method for calculating the δ^{53}Cr value of the BSE presented by Schoenberg *et al.* (2008)[25] and Xia *et al.* (2017),[47] and the sample types selected by Teng *et al.* (2004)[50] to evaluate the Li isotopic composition of the upper continental crust, we used a suite of granite,[25,28] diamictite,[51,52] loess[48] and stream sediments to estimate the Cr isotope composition of the upper crust. The δ^{53}Cr of these samples fall within a narrow range with an average of $-0.104 \pm 0.097‰$ (2SD, $n = 22$), which is within uncertainty the same as that of the BSE. Therefore, we suggested that the Cr isotopic composition in the upper continental crust is relatively homogeneous.

Ferromanganese nodules (NOD-P-1 and NOD-A-1) and cobalt-rich crusts (GSMC-2–3) are not only important mineral resources enriched in Co, Mn, Cu and Ni, but also potential geological archives for recording the information of marine environmental changes.[53–56] The Cr isotope composition of NOD-P-1 and NOD-A-1 is determined to be $-0.08 \pm 0.06‰$ and $0.03 \pm 0.06‰$, respectively. The latter is in accordance with the δ^{53}Cr ($0.07 \pm 0.09‰$, $n = 16$) reported by Gueguen *et al.* (2016),[17] whereas the δ^{53}Cr of GSMC-2 and -3 is $-0.32 \pm 0.06‰$ and $-0.37 \pm 0.06‰$, respectively. The NOD-P-1 and CSMC-2–3 were collected at 4300 m and 2000 m depths in the Pacific, while NOD-A-1 was

collected at a 788 m depth in the Atlantic. The different δ^{53}Cr among them may result from the heterogeneous distribution of Cr isotopic composition in the Ocean,[57,58] or reflect different isotope fractionation mechanisms during Cr incorporation into Fe–Mn nodules and Co-crusts. Since seawater generally has heavy Cr isotopic composition (+0.4% to +1.6%),[44,57,59] the adsorption of Cr does not seem to generate appreciable Cr isotope fractionation, and the −0.3‰ difference in δ^{53}Cr between Co-rich crusts and Fe–Mn nodules may be related to their different mineralogical and geochemical compositions.[60]

The δ^{53}Cr values of human hair (GSH-1) and plants (2 shrub leaves: GSV-1 and GSV-2; 1 spinach: GSB-6, and 1 tomato leaf: ESP-1) were determined to be −0.04 ± 0.06‰, −0.06 ± 0.06‰, −0.01 ± 0.06‰, 0.04 ± 0.06‰ and −0.03 ± 0.06‰, respectively. The average δ^{53}Cr of hair and plant samples (~0.1‰) is higher than that of soil, stream sediment and rock samples (Fig. 6). This observation is different from the isotopic compositions of Ni, Zn, and K in animal and plant samples,[61–63] which are lighter compared to rock samples. The slightly elevated δ^{53}Cr in biological samples suggests that the soluble Cr(VI) may be selectively taken up by tissues.

4. Conclusions

An improved, flexible three-step purification scheme with four column procedures was developed for obtaining high purity Cr from geological and environmental samples with low Cr content and complex matrices. In this scheme, Step I and Step II are designed to eliminate Fe (100%), Ca (>99%), Ti (>99%) and V (>90%) without Cr loss, even with very high ratios of Ti/Cr (1000) and Fe/Cr (9000). The recovery of Cr by our new method is generally high (80–99%). However, the yield for Fe–Mn nodules and human hair is slightly lower but still greater than 70%, likely due to low Cr content and more complex matrices. The Cr was mostly lost during loading onto the anion exchange resin after the oxidation step. The loss of Cr in manganese nodules was likely due to formation of a manganese oxide precipitate. Therefore, a higher Cr yield for manganese nodule samples may be achieved in future studies by removing Mn before the oxidation step or replacing the oxidation step with a cation separation procedure. The low yield in our human hair sample was due to directly performing Step III. A large sample matrix (~1 g sample) during oxidation likely leads to a relatively low oxidation efficiency.

Because the Cr yield has been improved and the blank was reduced to ≤1 ng, samples containing 300–600 ng of Cr were enough for highly precise and accurate measurement of Cr isotopes. The δ^{53}Cr of NIST SRM 979 and NIST SRM 3112a standards (either unprocessed or processed) was determined to be 0.00 ± 0.04‰ (2SD; n = 152) and −0.07± 0.04‰ (2SD; n = 29), consistent with previous determinations. The δ^{53}Cr of BHVO-2, JP-1, SDO-1 and JDO-1 was determined to be −0.12 ± 0.06‰ (2SD; n = 15), −0.09 ± 0.06‰ (2SD; n = 8), −0.05 ± 0.06‰ (2SD; n = 3), and 1.64 ± 0.06‰ (2SD; n = 3), again consistent with previous measurements.

Using our proposed separation protocol, we analyzed the Cr isotopic compositions of geological reference materials in the form of silicates, carbonates, soil, stream sediment, plants and human hair. Based on a selected suite of granite, loess, stream sediment and diamictite samples, the δ^{53}Cr of the upper crust was tentatively suggested to be −0.10 ± 0.10‰, which is indistinguishable from that of the BSE. The δ^{53}Cr of Co-rich crusts (−0.34 ± 0.06‰, n = 3) is significantly lower than that of Fe–Mn nodules (−0.03 ± 0.06‰, n = 2), possibly related to the different mineralogical and geochemical compositions between these two types of marine mineral deposits, although further investigation is needed. The δ^{53}Cr values for human hair and investigated plants are about 0.1‰ higher than that of the BSE, implying that biological tissues might selectively take up certain Cr species (*e.g.* Cr(VI)). In summary, these results suggest that our improved purification scheme can be applied to various kinds of geological and environmental samples.

Conflicts of interest

There are no conflicts of interest to declare.

Acknowledgements

This work was supported by the National Key Basic Research Program of China (2014CB238903) and the National Natural Science Foundation of China (Nos. 41473028, U1612441, and 41325010). We thank Dr Johnson at the University of Illinois for providing the calibrated double spike. Drs Robert Rudnick, Bing Shen and Xuefeng Sheng are greatly appreciated for providing diamictite and loess samples. The authors are also grateful for constructive comments and suggestions by two anonymous referees, and for editorial handling by Dr Ziva Whitelock.

References

1 J. R. de Laeter, J. K. Böhlke, P. De Bièvre, H. Hidaka, H. S. Peiser, K. J. R. Rosman and P. D. P. Taylor, *Pure Appl. Chem.*, 2003, **75**, 683–800.
2 J.-L. Birck and C. J. Allegre, *Nature*, 1988, **331**, 579–584.
3 A. Götz and K. G. Heumann, *Fresenius' Z. Anal. Chem.*, 1988, **331**, 123–128.
4 G. W. Lugmair and A. Shukolyukov, *Geochim. Cosmochim. Acta*, 1998, **62**, 2863–2886.
5 A. S. Ellis and T. D. Bullen, *Science*, 2002, **295**, 2060–2062.
6 S. Zink, R. Schoenberg and M. Staubwasser, *Geochim. Cosmochim. Acta*, 2010, **74**, 5729–5745.
7 R. Frei, C. Gaucher, S. W. Poulton and D. E. Canfield, *Nature*, 2009, **461**, 250–253.
8 D. B. Cole, C. T. Reinhard, X. Wang, B. Gueguen, G. P. Halverson, T. Gibson, M. S. W. Hodgskiss, N. R. Mckenzie, T. W. Lyons and N. J. Planavsky, *Geology*, 2016, **44**, G37781–G37787.
9 P. Bonnand, I. J. Parkinson, R. H. James, I. J. Fairchild and N. W. Rogers, *Geochim. Cosmochim. Acta*, 2009, **53**, 10–20.
10 J. Robles-Camacho and M. A. Armienta, *J. Geochem. Explor.*, 2000, **68**, 167–181.
11 N. Unceta, F. Séby, J. Malherbe and O. F. X. Donard, *Anal. Bioanal. Chem.*, 2010, **397**, 1097–1111.

12 J. A. Izbicki, J. W. Ball, T. D. Bullen and S. J. Sutley, *Appl. Geochem.*, 2008, **23**, 1325–1352.
13 R. E. Cranston and J. W. Murray, *Anal. Chim. Acta*, 1978, **99**, 275–282.
14 A. Basu and T. M. Johnson, *Environ. Sci. Technol.*, 2012, **46**, 244–4996.
15 J. D'Arcy, G. J. Gilleaudeau, S. Peralta, C. Gaucher and R. Frei, *Chem. Geol.*, 2017, **448**, 1–12.
16 J. D'Arcy, M. G. Babechuk, L. N. Døssing, C. Gaucher and R. Frei, *Geochim. Cosmochim. Acta*, 2016, **186**, 296–315.
17 B. Gueguen, C. T. Reinhard, T. J. Algeo, L. C. Peterson, S. G. Nielsen, X. Wang, H. Rowe and N. J. Planavsky, *Geochim. Cosmochim. Acta*, 2016, **184**, 1–19.
18 P. Bonnand, I. J. Parkinson and M. Anand, *Geochim. Cosmochim. Acta*, 2016, **175**, 208–221.
19 R. Schoenberg, A. Merdian, C. Holmden, I. C. Kleinhanns, K. Haßler, M. Wille and E. Reitter, *Geochim. Cosmochim. Acta*, 2016, **183**, 14–30.
20 M. Schiller, E. V. Kooten, J. C. Holst, M. B. Olsen and M. Bizzarro, *J. Anal. At. Spectrom.*, 2014, **29**, 1406–1416.
21 V. Chrastný, J. Rohovec, E. Čadková, J. Pašava, J. Farkaš and M. Novák, *Geostand. Geoanal. Res.*, 2013, **38**, 103–110.
22 P. Bonnand, I. J. Parkinson, R. H. James, A. M. Karjalainen and M. A. Fehr, *J. Anal. At. Spectrom.*, 2011, **26**, 528–535.
23 L. Qin, C. M. O. D. Alexander, R. W. Carlson, M. F. Horan and T. Yokoyama, *Geochim. Cosmochim. Acta*, 2010, **74**, 1122–1145.
24 A. Trinquier, J. L. Birck and C. J. Allègre, *J. Anal. At. Spectrom.*, 2008, **23**, 1565–1574.
25 R. Schoenberg, S. Zink, M. Staubwasser and F. von Blanckenburg, *Chem. Geol.*, 2008, **249**, 294–306.
26 L. Halicz, L. Yang, N. Teplyakov, A. Burg, R. Sturgeon and Y. Kolodny, *J. Anal. At. Spectrom.*, 2008, **23**, 1622–1627.
27 C. Li, L. Feng, X. Wang, Z. Y. Chu, J. H. Guo and S. A. Wilde, *J. Anal. At. Spectrom.*, 2016, **31**, 2375–2383.
28 C. Li, L. Feng, X. Wang, S. A. Wilde, Z. Y. Chu and J. H. Guo, *J. Anal. At. Spectrom.*, 2017, **32**, 1938–1945.
29 K. K. Larsen, D. Wielandt, M. Schiller and M. Bizzarro, *J. Chromatogr. A*, 2016, **1443**, 162–174.
30 S. G. John, *J. Anal. At. Spectrom.*, 2012, **27**, 2123–2131.
31 J. F. Rudge, B. C. Reynolds and B. Bourdon, *Chem. Geol.*, 2009, **265**, 420–431.
32 N. Dauphas, A. Pourmand and F. Z. Teng, *Chem. Geol.*, 2009, **267**, 175–184.
33 Y. He, S. Ke, F. Z. Teng, T. Wang, H. Wu, Y. Lu and S. Li, *Geostand. Geoanal. Res.*, 2015, **39**, 341–356.
34 T. M. Johnson, M. J. Herbel, T. D. Bullen and P. T. Zawislanski, *Geochim. Cosmochim. Acta*, 1999, **63**, 2775–2783.
35 S. Pontér, N. Pallavicini, E. Engström, D. C. Baxter and I. Rodushkin, *J. Anal. At. Spectrom.*, 2016, **31**, 1464–1471.
36 A. Yamakawa, K. Yamashita, A. Makishima and E. Nakamura, *Anal. Chem.*, 2009, **81**, 9787–9794.
37 F. Wombacher, A. Eisenhauer, A. Heuser and S. Weyer, *J. Anal. At. Spectrom.*, 2009, **24**, 627–636.
38 J. Zhang, N. Dauphas, A. M. Davis and A. Pourmand, *J. Anal. At. Spectrom.*, 2011, **26**, 2197–2205.
39 M. Bizzarro, C. Paton, K. Larsen, M. Schiller, A. Trinquier and D. Ulfbeck, *J. Anal. At. Spectrom.*, 2011, **26**, 565–577.
40 A. S. Rodler, S. V. Hohl, Q. Guo and R. Frei, *Chem. Geol.*, 2016, **436**, 24–34.
41 L. N. Døssing, K. Dideriksen, S. L. S. Stipp and R. Frei, *Chem. Geol.*, 2011, **285**, 157–166.
42 X. Wang, N. J. Planavsky, C. T. Reinhard, H. Zou, J. J. Ague, Y. Wu, B. C. Gill, E. M. Schwarzenbach and B. Peucker-Ehrenbrink, *Chem. Geol.*, 2016, **423**, 19–33.
43 P. Bonnand, H. M. Williams, I. J. Parkinson, B. J. Wood and A. N. Halliday, *Earth Planet. Sci. Lett.*, 2016, **435**, 14–21.
44 N. S. Pereira, A. R. Voegelin, C. Paulukat, A. N. Sial, V. P. Ferreira and R. Frei, *Geobiology*, 2016, **14**, 54–67.
45 G. J. Gilleaudeaur, R. Frei, A. J. Kaufman, L. C. Kah, K. Azmy, J. K. Bartley, P. Chernyavskiy and A. H. Knoll, *Geochemical Perspectives Letters*, 2016, **2**, 178–187.
46 W. Wu, X. Wang, C. T. Reinhard and N. J. Planavsky, *Chem. Geol.*, 2017, **456**, 98–111.
47 J. Xia, L. Qin, J. Shen, R. W. Carlson, D. A. Ionov and T. D. Mock, *Earth Planet. Sci. Lett.*, 2017, **464**, 103–115.
48 Y. Gong, Y. Xia, F. Huang and H. Yu, *Acta Geochim.*, 2017, **36**, 125–131.
49 R. Rudnick and S. Gao, *Treatise Geochem.*, 2003, **3**, 1–64.
50 F. Z. Teng, W. F. Mcdonough, R. L. Rudnick, C. Dalpe, P. B. Tomascak, B. W. Chappell and S. Gao, *Geochim. Cosmochim. Acta*, 2004, **68**, 4167–4178.
51 K. J. Huang, F. Z. Teng, B. Shen, S. Xiao, X. Lang, H. R. Ma, Y. Fu and Y. Peng, *Sci. Found. China*, 2017, **113**, 14904–14909.
52 R. M. Gaschnig, R. L. Rudnick, W. F. Mcdonough, A. J. Kaufman, J. W. Valley, Z. Hu, S. Gao and M. L. Beck, *Geochim. Cosmochim. Acta*, 2016, **186**, 316–343.
53 K. T. Goto, A. D. Anbar, G. W. Gordon, S. J. Romaniello, G. Shimoda, Y. Takaya, A. Tokumaru, T. Nozaki, K. Suzuki and S. Machida, *Geochim. Cosmochim. Acta*, 2014, **146**, 43–58.
54 X. Wang, N. J. Planavsky, C. T. Reinhard, J. R. Hein and T. M. Johnson, *Am. J. Sci.*, 2016, **316**, 64–83.
55 J. R. Hein, W. A. Bohrson, M. S. Schulz, M. Noble and D. A. Clague, *Paleoceanography*, 1992, **7**, 63–77.
56 G. M. Mcmurtry, D. L. Vonderhaar, A. Eisenhauer, J. J. Mahoney and H. W. Yeh, *Earth Planet. Sci. Lett.s*, 1994, **125**, 105–118.
57 K. Scheiderich, M. Amini, C. Holmden and R. Francois, *Earth Planet. Sci. Lett.*, 2015, **423**, 87–97.
58 C. Paulukat, G. J. Gilleaudeau, P. Chernyavskiy and R. Frei, *Chem. Geol.*, 2016, **444**, 101–109.
59 P. Bonnand, R. H. James, I. J. Parkinson, D. P. Connelly and I. J. Fairchild, *Earth Planet. Sci. Lett.*, 2013, **382**, 10–20.
60 J. R. Hein, A. Koschinsky, M. Bau, F. T. Manheim, J.-K. Kang and L. Roberts, *Handbook of marine mineral deposits*, 1999, pp. 239–280.
61 D. J. Weiss, T. F. D. Mason, F. J. Zhao, G. J. D. Kirk, B. J. Coles and M. S. A. Horstwood, *New Phytol.*, 2005, **165**, 703–710.
62 T.-H.-B. Deng, C. Cloquet, Y.-T. Tang, T. Sterckeman, G. Echevarria, N. Estrade, J.-L. Morel and R.-L. Qiu, *Environ. Sci. Technol.*, 2014, **48**, 11926–11933.
63 W. Li, B. L. Beard and S. Li, *J. Anal. At. Spectrom.*, 2016, **31**, 1023–1029.